JACS
JOURNAL OF THE AMERICAN CHEMICAL SOCIETY

Article

pubs.acs.org/JACS

Spray Drying for Making Covalent Chemistry: Postsynthetic Modification of Metal–Organic Frameworks

Luis Garzón-Tovar,[†] Sabina Rodríguez-Hermida,[†] Inhar Imaz,[†] and Daniel Maspoch*[,†,‡]

[†]Catalan Institute of Nanoscience and Nanotechnology (ICN2), CSIC and The Barcelona Institute of Science and Technology, Campus UAB, Bellaterra, 08193 Barcelona, Spain

[‡]ICREA, Pg. Lluís Companys 23, 08010 Barcelona, Spain

Supporting Information

ABSTRACT: Covalent postsynthetic modification (PSM) of metal–organic frameworks (MOFs) has attracted much attention due to the possibility of tailoring the properties of these porous materials. Schiff-base condensation between an amine and an aldehyde is one of the most common reactions in the PSM of MOFs. Here, we report the use of the spray drying technique to perform this class of organic reactions, either between discrete organic molecules or on the pore surfaces of MOFs, in a very fast (1–2 s) and continuous way. Using spray drying, we show the PSM of two MOFs, the amine-terminated UiO-66-NH_2 and the aldehyde-terminated ZIF-90, achieving conversion efficiencies up to 20 and 42%, respectively. Moreover, we demonstrate that it can also be used to postsynthetically cross-link the aldehyde groups of ZIF-90 using a diamine molecule with a conversion efficiency of 70%.

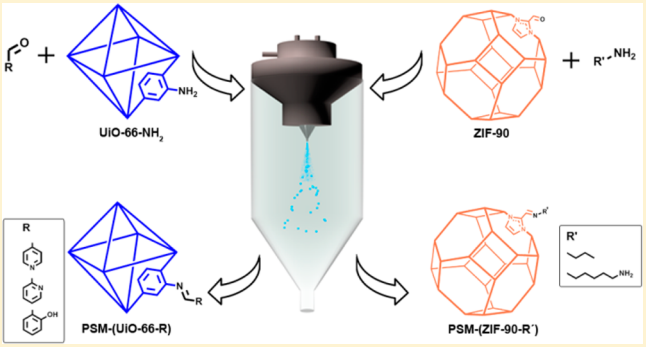

INTRODUCTION

Metal–organic frameworks (MOFs), also known as porous coordination polymers (PCPs), have attracted much attention over the past decades due to their potential applications, such as in gas sorption and storage, catalysis, drug delivery, and gas separation.[1−3] One of the main characteristics of MOFs is the ability to tailor their chemical functionality and/or pore surface chemistry, either by pre- or postsynthetic modification of the organic linker. Covalent postsynthetic modification (PSM) involves an organic reaction carried out on the organic linker while maintaining the MOF integrity.[4,5]

To date, there are many studies based on the PSM of MOFs involving linkers with different functional groups.[6−9] Among them, the most common reaction involves a Schiff-base condensation between an amine and an aldehyde to form an imine via water elimination. Using this chemistry, PSM of the 2-aminoterephthalate (NH_2-bdc) linker of UiO-66-NH_2 has been widely studied.[10−16] For example, Lu et al. showed the successful PSM of UiO-66-NH_2 with salicylaldehyde (Sal) by heating a mixture of both species in acetonitrile at 40 °C for 3 days. Once functionalized, they further immobilized Cu(II) salts on the incorporated imine moiety, and used the resulting framework as an efficient catalyst for the aerobic oxidation of alcohols.[10] A similar strategy was also followed to synthesize efficient catalysts for the epoxidation of olefins, the hydrogenation of aromatics, and the reductive amination of aldehydes.[11−13] In these cases, UiO-66-NH_2 was postsynthetically modified with Sal, 2-pyridinecarboxaldehyde, 4-pyridinecarboxaldehyde, and 6-((diisopropylamino)methyl)-picolinaldehyde followed by the immobilization of Mo(VI) and Ir(I). Also, other amino-terminated MOFs such as IRMOF-3 and Cr-MIL-101-NH_2 have been used for the development of efficient catalysts. Here, both MOFs were first reacted with pyridine-based aldehydes and then with Cu(I) and Co(II) salts to create heterogeneous catalysts for the synthesis of different 2-aminobenzothiazoles and the aerobic epoxidation of olefins, respectively.[14,15]

Yaghi et al. also reported the use of the Schiff-base condensation reaction to postsynthetically functionalize aldehyde-terminated MOFs. They reacted ZIF-90 with ethanolamine, yielding the imine-derivative nonporous ZIF-92.[17] Following the same type of chemistry, ZIF-90 was recently labeled with an Alexa Fluor dye,[18] whereas a mixed ZIF-8-90 sample was postfunctionalized with ethylenediamine. This latter PSM allowed the introduction of an aliphatic amine-terminated group to ZIF-8-90, enhancing its CO_2 sorption capacity.[19] In a more recent study, a superhydrophobic ZIF-90 exhibiting a water contact angle value of around 152° was prepared by reacting it with a polyfluorinated amine.[20]

In general, the synthetic conditions for the PSM of MOFs require long reactions times (from 1 to 3 days) and high temperatures. To overcome these limitations, some advances have been done on developing alternative methods for the PSM of MOFs. One of them is based on the PSM of IRMOF-3 and UiO-66-NH_2 by vapor diffusion.[21] This method allowed the

Received: October 28, 2016
Published: January 3, 2017

DOI: 10.1021/jacs.6b11240
J. Am. Chem. Soc. 2017, 139, 897–903

PSM of both MOFs with high conversion rates after heating the solvent-free MOFs with the corresponding aldehyde at 100–120 °C using a vacuum system for 16 h.

Recently, it has been demonstrated that the spray drying (SD) technique is a useful, continuous, and scalable method to assemble metal ions and organic ligands to synthesize MOFs.[22,23] This method allowed the reaction times to be drastically reduced down to the second regime, without affecting the properties of the SD-synthesized MOFs. It also enables obtaining them in the form of dried powders and recycling the solvent used during the fabrication. Here, we extended the use of SD to covalent organic reactions based on the Schiff-base condensation reaction aiming to be able to postsynthetically modify MOF crystals. UiO-66-NH_2 and ZIF-90 were selected as the target MOFs due to the uncoordinated and available amine and aldehyde groups within their structures, respectively (Scheme 1).

Scheme 1. Illustration of the Covalent PSM Performed in (a) UiO-66-NH_2 and (b) ZIF-90 under SD Conditions

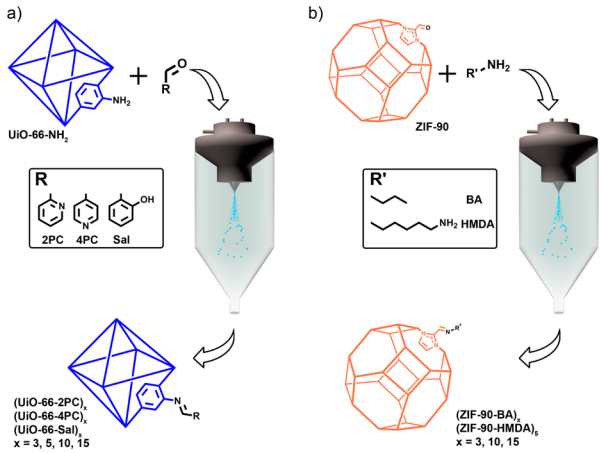

RESULTS AND DISCUSSION

Organic Schiff-Base Condensation Reactions Conducted via Spray Drying. To demonstrate that organic reactions and, in particular, Schiff-base condensation reactions between aldehydes and amines could be performed using the SD technique, we initially tested the formation of 2-((pyridin-4-ylmethylene)amino)terephthalic acid using NH_2-bdc and 4-pyridinecarboxaldehyde (4PC) as reactants (Scheme 2). This synthesis started with the mixture of NH_2-bdc and 4PC in ethanol (15 mL) at room temperature. The NH_2-bdc:4PC molar ratio was systematically changed from 1:1, 1:2, and 1:3. Each suspension was then spray-dried at a feed rate of 3.0 mL min^{-1} and an inlet temperature of 130 °C, using a Mini Spray Dryer B-290. This inlet temperature was selected to ensure the evaporation of ethanol as well as to force the evaporation of the water formed during the Schiff-base condensation reaction. For each reaction, a yellow powder was collected after 5 min. ^{1}H NMR spectra of all collected powders confirmed the imine formation by the appearance of a peak at 8.17 ppm corresponding to the imine proton (Figures 1a and S1). The synthesis of 2-((pyridin-4-ylmethylene)amino)terephthalic acid was further corroborated by ^{13}C NMR (peak corresponding to the carbon atom of the CH═N imine group at 163 ppm; Figures 1b and S2) and ESI-MS (calculated for $[M\text{-}H]^-$ $[C_{14}H_9N_2O_4]^-$: m/z = 269.0568; found m/z = 269.0566; Figure S3). We finally determined the conversion rate of each reaction by comparing the integration of the peaks at 8.17 ppm (imine proton) and at 7.02 ppm (aromatic proton of the unreacted NH_2-bdc). The conversion rates were 37, 84, and 92% for the NH_2-bdc:4PC molar ratios of 1:1, 1:2, and 1:3, respectively.

Scheme 2. Imine Molecules Synthesized *via* SD

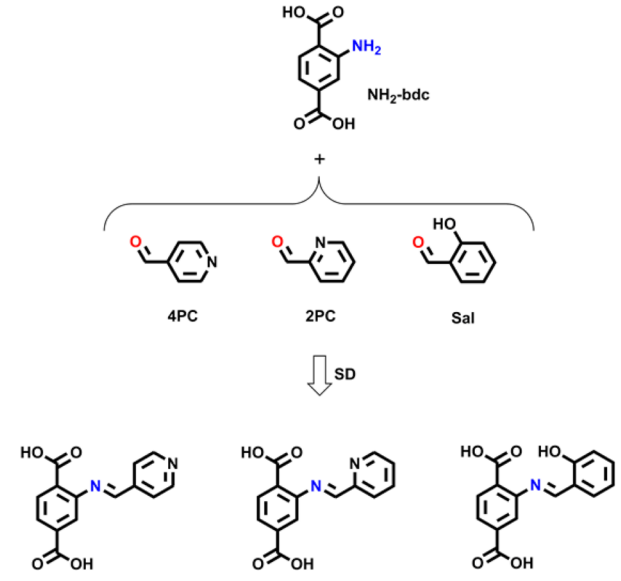

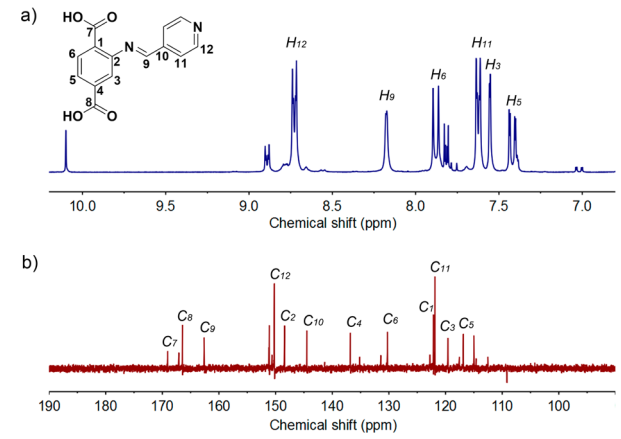

Figure 1. (a) ^{1}H NMR and (b) ^{13}C NMR spectra, collected in DMSO-d_6, of 2-((pyridin-4-ylmethylene)amino)terephthalic acid synthesized using a NH_2-bdc:4PC molar ratio of 1:3. Only the peaks corresponding to the imine molecule are shown.

We then extended the SD synthesis to two other imine compounds (Scheme 2). The syntheses were done using the same conditions as those for 2-((pyridin-4-ylmethylene)-amino)terephthalic acid, except that, instead of 4PC, we used 2-pyridinecarboxaldehyde (2PC; conversion rate: 87%) and Sal (conversion rate: 75%) in a NH_2-bdc:2PC/Sal molar ratio of 1:3. In both cases, the expected imine compounds were successfully synthesized, as confirmed by ^{1}H and ^{13}C NMR and ESI-MS (Figures S4–S9).

The high conversion rates obtained in these Schiff-base condensation reactions are remarkable if we consider that, to the best of our knowledge, this is the first time that discrete organic molecules have been synthesized via SD. It is well-known that, in these condensation reactions, water is produced so that its removal favors the formation of imines following the

DOI: 10.1021/jacs.6b11240
J. Am. Chem. Soc. 2017, 139, 897–903

Le Chatelier principle. Since SD is based on the fast evaporation of the liquid, we reason that water can be rapidly removed from the atomized droplets during the Schiff-base reaction, thereby favoring the formation of the imine bond.

PSM of UiO-66-NH_2. Once we proved the SD synthesis of imine compounds via Schiff-base condensation, we then transferred the same type of chemistry to MOF crystals. For this, we selected UiO-66-NH_2 as the first test case scenario because the amino groups of the NH_2-bdc linkers are pointing into the pores, and of its high chemical and thermal stability.

A series of ethanolic colloidal suspensions (15 mL) containing UiO-66-NH_2 [synthesized under solvothermal conditions; particle size = 245 ± 65 nm; obtained as pure phase as confirmed by X-ray powder diffraction (XRPD), scanning electron microscopy (SEM), N_2 sorption isotherm (S_{BET} = 914 m^2 g^{-1}), and ^{13}C MAS NMR; see Figures S10–S12] and the aldehydes 4PC, 2PC, and Sal were initially prepared at molar ratios of NH_2-bdc:aldehyde corresponding to 1:3, 1:5, 1:10, and 1:15. Each suspension was then spray-dried under the same conditions as those for the pure condensation SD reactions. Once the suspensions had atomized, the different yellow powders were collected from the spray dryer collector, cleaned with ethanol four times and once with acetone, and finally dried at 85 °C for 12 h. The different samples were named as $(UiO\text{-}66\text{-}4PC)_x$, $(UiO\text{-}66\text{-}2PC)_x$, and $(UiO\text{-}66\text{-}Sal)_x$ (where x is 3, 5, 10, and 15, depending on the equivalents of aldehyde used). Field-emission scanning electron microscopy (FESEM) of all dried powders revealed that the initial size and morphology of the parent UiO-66-NH_2 crystals did not change during the SD process (Figure S13). XRPD indicated that all crystalline powders retain the crystallinity of the parent UiO-66-NH_2 MOF (Figures 2b and S14–S16).

To confirm the PSM of UiO-66-NH_2 with the different aldehydes, we first performed ^{13}C MAS NMR on $(UiO\text{-}66\text{-}2PC)_{15}$, $(UiO\text{-}66\text{-}4PC)_{15}$, and $(UiO\text{-}66\text{-}Sal)_{15}$ (Figures 2a and S17–S19). All spectra showed the appearance of a new signal centered at 160–161 ppm, which was attributed to the carbon atom of the CH═N imine group. This peak is consistent with the one observed at 160–162 ppm in the ^{13}C NMR spectra of the imine compounds previously synthesized via SD (Figures S2, S5, and S8). It is also in agreement with the ^{13}C MAS NMR signal associated with the imine carbon in other reported postfunctionalized UiOs.[11,12]

The degree of postsynthetic conversion was analyzed by first digesting the samples and then analyzing the resulting solutions by ^1H NMR. From the digestion under acidic conditions, the MOF framework is destroyed and the released imine molecules are hydrolyzed forming the NH_2-bdc and the corresponding aldehyde. We then calculated the conversion rate by comparison of the integration of one peak at 7.36 ppm corresponding to NH_2-bdc and those peaks at 7.98, 8.52, and 7.52 ppm corresponding to 4PC, 2PC, and Sal, respectively (Figures S20–S32). Also note here that all samples were previously washed three times with ethanol and acetone, and then dried at 85 °C overnight before their digestion. This activation process ensures the removal of all nonreacted aldehyde molecules adsorbed in the pores of the MOFs during the SD process, as confirmed by FT-IR (Figures S33–S35). Table 1 lists the degrees of conversion calculated for all synthesized samples. From this data, it was clear that the degree of conversion increases while increasing the equivalents of aldehyde used in the reaction.

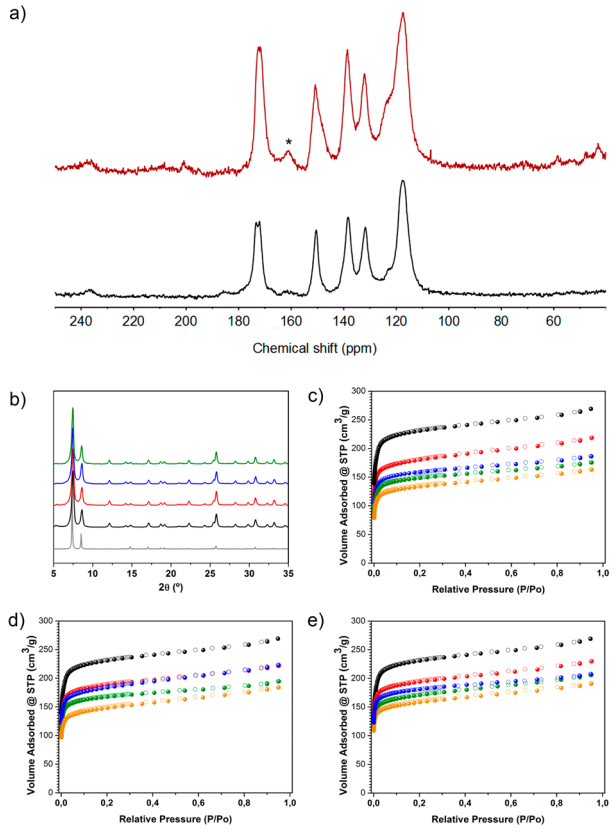

Figure 2. (a) ^{13}C MAS NMR spectra of $(UiO\text{-}66\text{-}2PC)_{15}$ (red) and UiO-66-NH_2 (black). The signal of the CH═N imine group is highlighted with an asterisk (*). (b) XRPD patterns of simulated UiO-66-NH_2 (gray) and activated UiO-66-NH_2 (black), $(UiO\text{-}66\text{-}2PC)_{15}$ (red), $(UiO\text{-}66\text{-}4PC)_{15}$ (blue), and $(UiO\text{-}66\text{-}Sal)_{15}$ (green). (c–e) N_2 sorption isotherms of (c) $(UiO\text{-}66\text{-}2PC)_x$, (d) $(UiO\text{-}66\text{-}4PC)_x$, and (e) $(UiO\text{-}66\text{-}Sal)_x$ synthesized with different equivalents of aldehyde (x). In parts c–e, x = 3 (red), x = 5 (blue), x = 10 (green), and x = 15 (orange). For comparison, N_2 sorption isotherms of activated UiO-66-NH_2 (black) are also included.

Table 1. BET Areas, Pore Volumes, and % of Conversion of UiO-66-NH_2, $(UiO\text{-}66\text{-}2PC)_x$, $(UiO\text{-}66\text{-}4PC)_x$, and $(UiO\text{-}66\text{-}Sal)_x$

MOF	x	S_{BET} (m^2 g^{-1})	pore vol.[a] (cm^3 g^{-1})	conversion[b] (%)
UiO-66-NH_2		914	0.3729	
$(UiO\text{-}66\text{-}2PC)_x$	3	699	0.2954	13
	5	625	0.2576	16
	10	586	0.2412	17
	15	516	0.2190	20
$(UiO\text{-}66\text{-}4PC)_x$	3	736	0.3056	9
	5	712	0.3015	16
	10	621	0.2652	18
	15	573	0.2441	20
$(UiO\text{-}66\text{-}Sal)_x$	3	761	0.3151	11
	5	709	0.2923	14
	10	665	0.2789	16
	15	616	0.2587	19

[a]Calculated at $P/P_0 \approx 0.4$. [b]Calculated from ^1H NMR spectra of the digested samples.

For example, the degree of conversion increased from 13 to 20% between $(UiO\text{-}66\text{-}2PC)_3$ and $(UiO\text{-}66\text{-}2PC)_{15}$. It is

DOI: 10.1021/jacs.6b11240
J. Am. Chem. Soc. 2017, 139, 897–903

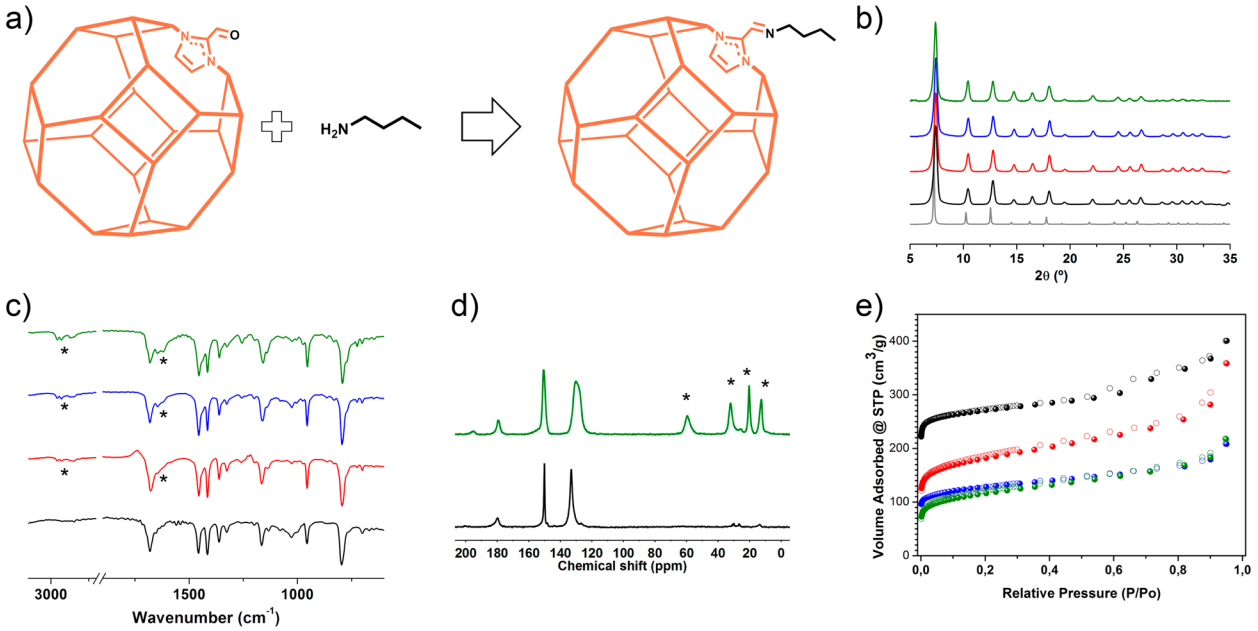

Figure 3. (a) Schematic representation of the PSM of ZIF-90 with butylamine via SD. (b) XRPD patterns of ZIF-90 and $(ZIF\text{-}90\text{-}BA)_x$, as compared to the simulated powder pattern for the crystal structure of ZIF-90 (gray). (c) IR spectra of ZIF-90 and $(ZIF\text{-}90\text{-}BA)_x$, highlighting the aliphatic C—H and imine C═N vibrational bands with an asterisk (*). (d) ^{13}C MAS NMR spectra of ZIF-90 and $(ZIF\text{-}90\text{-}BA)_{15}$, where the peaks corresponding to the butyl chains are highlighted with an asterisk (*). (e) N_2 sorption isotherms at 77 K of ZIF-90 and $(ZIF\text{-}90\text{-}BA)_x$. In parts b–e, ZIF-90 (black), $(ZIF\text{-}90\text{-}BA)_3$ (red), $(ZIF\text{-}90\text{-}BA)_{10}$ (blue), and $(ZIF\text{-}90\text{-}BA)_{15}$ (green).

important to highlight here that the degree of conversion achieved by SD is higher than the ones reported for the PSM of UiO-66-NH_2 with the same aromatic aldehydes.[10,13] The only exception was the conversion rate of 29% reported by Bokhoven and co-workers for the formation of (UiO-66-Sal) via the vapor-phase method.[21] However, this latter method is a noncontinuous method, which requires a vacuum and 16 h to achieve this conversion rate.

N_2 sorption isotherms were finally measured at 77 K on all activated samples that were further degassed at 200 °C for 12 h under a vacuum. We found that the surface area and pore volumes decreased for the samples showing a higher degree of conversion (Table 1, Figures 2c–e and S36–S47). We attributed this trend to the fact that the new imine moieties grafted on the pores are bulkier than the amino group.

PSM of ZIF-90. To explore the versatility of the PSM via SD, we then switched to a terminal aldehyde-containing MOF to postfunctionalize it with amine molecules. To this end, we selected ZIF-90 that is built up from imidazole-2-carboxaldehyde (ICA) and Zn(II) ions, giving rise to a **sod**-3D porous network showing a pore size around 11 Å and a pore size window around 3.5 Å. Following a similar synthetic procedure as that for the PSM of UiO-66-NH_2, three ethanolic suspensions of ZIF-90 [synthesized at room temperature; particle size = 41 ± 9 nm; obtained as pure phase as confirmed by XRPD, SEM, N_2 sorption isotherm (S_{BET} = 1070 m^2 g^{-1}), and ^{13}C MAS NMR; see Figures S48–S50] and butylamine (BA) were initially prepared at molar ratios of ICA:BA corresponding to 1:3, 1:10, and 1:15. Each suspension was then spray-dried under the same above-mentioned conditions. Once the suspensions had atomized, the different pale yellow powders were collected from the spray dryer collector, cleaned with ethanol five times and once with acetone, and finally dried at 85 °C for 12 h. Again, the resulting powders were named as $(ZIF\text{-}90\text{-}BA)_x$, where x is the number of equivalents of BA.

Similarly, FESEM and TEM revealed that the initial size and morphology of the parent ZIF-90 crystals did not change during the SD process (Figure S51), whereas XRPD indicated that all crystalline powders retain the parent **sod** structure (Figures 3b and S52). In this case, the formation of imidazol-2-butylmethanimine (IBI) was initially confirmed by FT-IR spectroscopy. Two sets of new bands appeared in the IR spectra of the postsynthetic functionalized ZIF-90 (Figure 3c): (1) the band corresponding to the C═N group, centered at ≈1644 cm^{-1}, whose intensity increased as the equivalents of BA were increased, and (2) the aliphatic C—H stretching of the butyl moiety within the 3000–2700 cm^{-1} range. Moreover, no band corresponding to —NH_2 was observed, indicating that there was not unreacted BA inside the pores of ZIF-90. The formation of IBI was further corroborated by the peaks observed in the ^{13}C MAS NMR spectra at 59, 32, 20, and 13 ppm, which were all attributed to the butyl chain (Figure 3d). The peak at 59 ppm was assigned to the methylene group bonded to imine nitrogen. Moreover, the signal of the aldehyde group was observed at 195 ppm, indicating that not all carbonyl groups were reacted. Finally, the formation of IBI was undoubtedly confirmed by identifying it in the solution resulting from dissolving all $(ZIF\text{-}90\text{-}BA)_x$ samples using acetic acid (Figures S53–S55). Indeed, ^1H NMR spectra showed peaks at 8.55 and 3.82 ppm that were attributed to the CH═N imine proton and the N—CH_2 methylene protons of IBI, respectively. On the other hand, the peak at m/z = 152.1180 in the ESI-MS spectra matches with the molecular formula of the protonated IBI $[C_8H_{13}N_3]^+$ (m/z = 152.1182). Note here that, under these conditions, IBI was also partially hydrolyzed.

In order to quantify the conversion rate, ^1H NMR spectra of the digested samples in DCl, DMSO-d_6 were collected (Figure S56–S59). Under these stronger acidic conditions, ZIF-90 is dissolved and the released IBI is completely hydrolyzed, forming ICA and BA. Thus, the degree of conversion was

DOI: 10.1021/jacs.6b11240
J. Am. Chem. Soc. 2017, 139, 897–903

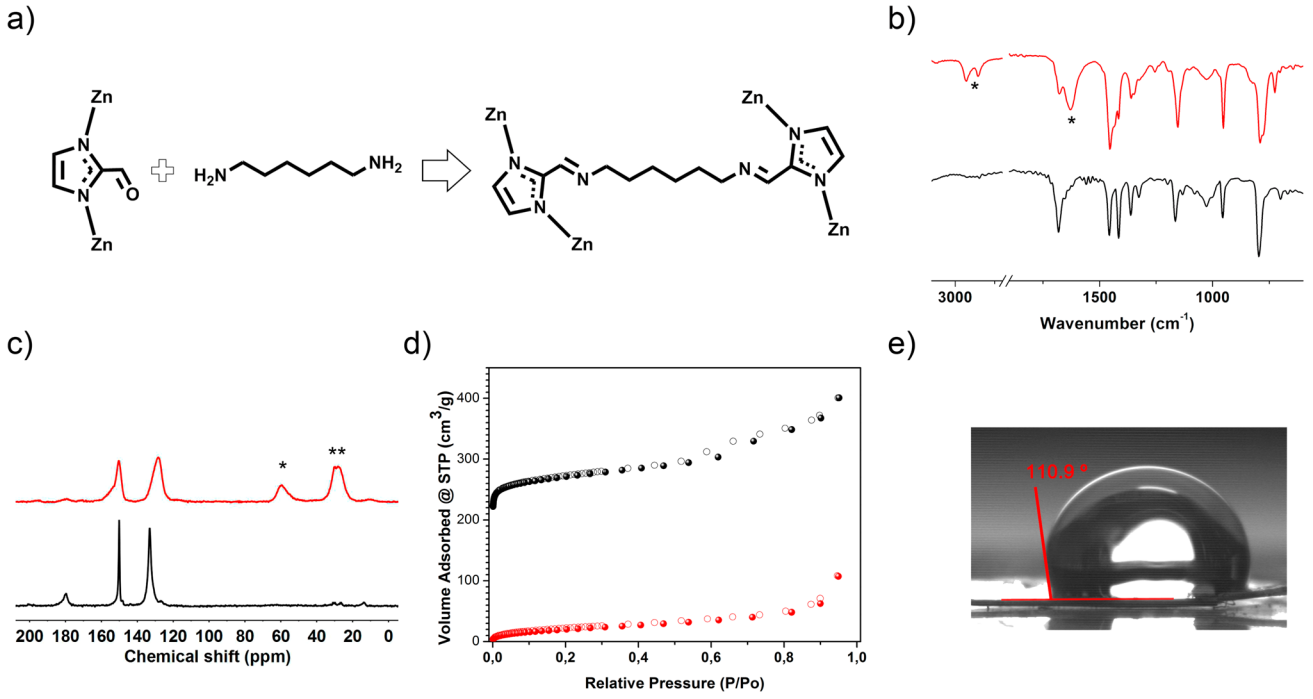

Figure 4. (a) Schematic representation of the PSM of ZIF-90 with hexamethylenediamine. (b) IR spectra of ZIF-90 (black) and $(ZIF\text{-}90\text{-}HMDA)_5$ (red), highlighting the aliphatic C—H and imine C═N vibrational bands with an asterisk (*). (c) ^{13}C MAS NMR spectra of ZIF-90 (black) and $(ZIF\text{-}90\text{-}HMDA)_5$ (red), where the peaks at the alkyl region are highlighted with an asterisk (*). (d) N_2 sorption isotherms of ZIF-90 (black) and $(ZIF\text{-}90\text{-}HMDA)_5$ (red). (e) Contact angle image of a pressed pellet disk of $(ZIF\text{-}90\text{-}HMDA)_5$.

measured by comparison of the integration of the peaks at 7.57 and 0.86 ppm corresponding to ICA and BA, respectively. We found that the conversion rates were 25% for $(ZIF\text{-}90\text{-}BA)_3$, 32% for $(ZIF\text{-}90\text{-}BA)_{10}$, and 42% for $(ZIF\text{-}90\text{-}BA)_{15}$.

These results were consistent with the gradual decrease of the S_{BET} values (determined by the N_2 sorption isotherms at 77 K) as the conversion rate (introduction of more bulky butyl chains) was also increased (Figures 3e and S60–S62). The calculated S_{BET} values were 670, 483, and 424 $m^2\ g^{-1}$ for $(ZIF\text{-}90\text{-}BA)_3$, $(ZIF\text{-}90\text{-}BA)_{10}$, and $(ZIF\text{-}90\text{-}BA)_{15}$, respectively. These values corresponded to a loss of 39, 45, and 63% of the S_{BET} of the parent ZIF-90.

Previous studies have shown that the introduction of alkyl chains in the pore surfaces of a MOF increases its hydrophobicity.[24,25] We therefore studied the surface wettability of all postfunctionalized ZIF-90 samples by measuring the contact angle (Θ_c) on pressed pellet disks of ZIF-90, $(ZIF\text{-}90\text{-}BA)_3$, $(ZIF\text{-}90\text{-}BA)_{10}$, and $(ZIF\text{-}90\text{-}BA)_{15}$. The Θ_c in each case was 90.4, 93.3, 96.1, and 99.3°, respectively—confirming an increase in the hydrophobicity when the conversion rate increases (Figure S63).

Finally, the effect of the particle size on this spray drying solid/liquid reaction was studied. To this end, suspensions containing larger ZIF-90 crystals (particle size: 18 ± 9 μm, Figures S64–S65) and ICA (using ICA:BA 1:15 molar ratio) were spray-dried under the same experimental conditions as described above, *vide supra*. Here, a conversion rate of 22% was determined by analyzing the ^1H NMR spectra of the digested sample (Figure S66). This value is lower than the one obtained when ZIF-90 nanoparticles were used (42%), and it is comparable to other conversion rates found in aldehyde-terminated ZIF particles of similar size.[25,26]

PSM of ZIF-90 with a Diamine Molecule. We further evaluated the PSM via SD by using hexamethylenediamine (HMDA) to cross-link nearby aldehyde groups located on the pores of ZIF-90 (Figure 4a). It is important to mention here that PSMs of ZIFs with terminal and aliphatic diamine molecules, such as ethylenediamine, have already been reported. For example, Balkus and co-workers cross-linked neighboring SIM-1 crystals with ethylenediamine to form a highly compact selective water/methanol membrane.[27]

Following the procedure applied in the previous PSMs via SD, an ethanolic suspension of ZIF-90 and HMDA (molar ratio aldehyde:amine = 1:5) was spray-dried under the same above-mentioned conditions. The collected powder called $(ZIF\text{-}90\text{-}HMDA)_5$ was also cleaned with ethanol five times and once with acetone, and dried at 85 °C for 12 h. Again, we did not observe any significant change in the crystal size and morphology during the SD process (Figure S67), and the XRPD indicated that the collected crystals retain the parent ZIF-90 structure (Figure S68).

The FT-IR spectrum of $(ZIF\text{-}90\text{-}HMDA)_5$ showed the presence of the characteristic C—H stretching bands of the hexamethyl chains at 2930 and 2850 cm^{-1} as well as a new band centered at 1630 cm^{-1} corresponding to the C═N group (Figure 4b). Moreover, the absence of the characteristic vibrational bands of the NH_2 groups suggested that both amino groups of the HMDA were reacted. Altogether these observations agree well with an effective cross-linking of the aldehyde groups located on the pores of ZIF-90 using HMDA.

We further studied this cross-linking by ^{13}C MAS NMR. The spectrum of $(ZIF\text{-}90\text{-}HMDA)_5$ showed a low intensity of the peak at 179 ppm corresponding to the aldehyde group, suggesting a low concentration of this group within the framework (Figure 4c). This result agrees well with the FT-IR spectrum, in which a low intensity of the band at 1675 cm^{-1} corresponding to the aldehyde group was also observed (Figure 4b). On the other hand, three signals in the alkyl region (60, 30,

DOI: 10.1021/jacs.6b11240
J. Am. Chem. Soc. 2017, 139, 897–903

and 27 ppm) were observed, indicating high symmetry in (ZIF-90-HMDA)$_5$. The downfield signal was attributed to the —N=CH_2— methylene groups, and the other two signals to the four —CH_2— methylene groups of the diimine bridge. In fact, we did not detect the characteristic peak of the —CH_2—NH_2 methylene centered at ≈40 ppm,[19] which would indicate that HMDA was only attached by one of its amine groups. The presence of the diimine cross-linking molecule *N,N′*-(hexane-1,6-diyl)bis(1-imidazol-2-yl)methanimine) (Figure 4a) was finally confirmed by analyzing the solution resulting from the digestion of (ZIF-90-HMDA)$_5$ in acetic acid by ^{1}H NMR and ESI-MS (Figure S69). The peaks at 8.58 and 3.83 ppm in the ^{1}H NMR spectrum were attributed to the CH=N imine proton and the N—CH_2 methylene protons of the diamine molecule, respectively. On the other hand, in the ESI-MS spectra, the peak at m/z = 273.1836 matches with the molecular formula of the protonated *N,N′*-(hexane-1,6-diyl)-bis(1-imidazol-2-yl)methanimine) $[C_{14}H_{20}N_6]^+$ (m/z = 273.1822).

The ^{1}H NMR spectrum of the digested (ZIF-90-HMDA)$_5$ in strong acidic conditions (DCl, DMSO-d_6) was collected to quantify its yield of conversion (Figure S70). Comparison of the integration of the signals corresponding to ICA (7.56 ppm) and HMDA (1.30 ppm) revealed that there is 35% HMDA, meaning that 70% of the ICA linkers were functionalized.

This high conversion of cross-linked ICA linkers in (ZIF-90-HMDA)$_5$ should therefore involve a remarkable closure of its pores and reduction of its surface area in comparison to its parent ZIF-90. This assumption was confirmed by measuring the S_{BET} from the N_2 sorption isotherm at 77 K. We found a S_{BET} of 69 m^2 g^{-1} that corresponds to a reduction of 93% of the original S_{BET} of ZIF-90 (Table 2, Figures 4d and S71).

Table 2. BET Areas, Pore Volumes, and % of Conversion of ZIF-90, (ZIF-90-BA)$_x$, and (ZIF-90-HMDA)$_5$

MOF	x	S_{BET} (m^2 g^{-1})	pore vol.[a] (cm^3 g^{-1})	conver.[b] (%)
ZIF-90		1070	0.4412	
(ZIF-90-BA)$_x$	3	670	0.3150	25
	10	483	0.2166	32
	15	424	0.2042	42
(ZIF-90-HMDA)$_5$	5	69	0.0377	70

[a]Calculated at P/P_0 ≈ 0.4. [b]Calculated from ^{1}H NMR spectra of the digested samples.

The contact angle (Θ_c) was also measured on a pressed pellet disk of (ZIF-90-HMDA)$_5$, giving a value of 110.9° that corresponds to a higher hydrophobic surface in comparison to the different (ZIF-90-BA)$_x$ samples (Figure 4e).

CONCLUSIONS

We have reported a highly versatile and effective methodology to postsynthetically modify MOFs via Schiff-base condensation reactions. This strategy can be applied to MOFs with either terminal aldehyde or amine groups, reduces their PSM time, and enables their continuous PSM with good rates of conversion. Therefore, it should facilitate the PSM of MOFs for numerous applications, including catalysis, sensor technology, pollutant removal, and separation. This method also allowed the efficient cross-linking of the terminal aldehydes groups of ZIF-90 using a diamine molecule, thereby blocking their porosity and opening up new avenues for future triggered delivery systems. Finally, it also enables performing Schiff-base condensation reactions between discrete amine and aldehyde molecules, opening new perspectives in organic chemistry synthesis.

MATERIALS AND METHODS

General Procedure for Synthesis of Imine Ligands. In a typical synthesis, a suspension of NH_2-bdc and the corresponding aldehyde (4PC, 2PC, and Sal) in 15 mL of ethanol was spray-dried at an inlet temperature of 130 °C, a feed rate of 3.0 mL min^{-1}, and a flow rate of 336 mL min^{-1} using a Mini Spray Dryer B-290 (BÜCHI Labortechnik; spray cap: 0.5 mm hole). The collected solids were characterized by ESI-MS, and ^{1}H- and ^{13}C NMR spectroscopy. Full experimental details and characterization can be found in the Supporting Information.

Synthesis of UiO-66-NH_2. UiO-66-NH_2 was synthesized through the previously reported method.[28] In a typical synthesis, 35 mL of HCl 37% was added to a solution 0.1 M $ZrCl_4$ and 0.1 M NH_2-bdc in 500 mL of DMF. The resulting mixture was heated at 120 °C under stirring for 2 h. The obtained solid was collected by centrifugation and washed two times with 100 mL of DMF for 12 h at 120 °C and three times with 100 mL of absolute ethanol for 12 h at 60 °C. Finally, the resulting powder was dried at 85 °C overnight (yield = 75%). Characterization details can be found in the Supporting Information.

Synthesis of ZIF-90. ZIF-90 was synthesized through the previously reported method.[18] In a typical synthesis, 0.27 mL of trimethylamine (1.96 mmol) was added to a solution 0.01 M imidazole-2-carboxaldehyde and 3.75 mM $Zn(NO_3)_2{\cdot}6H_2O$ in 200 mL of DMF. The resulting mixture was stirred for 1 min at room temperature, and then, 100 mL of ethanol was added. The particles were collected by centrifugation, washed five times with ethanol and one time with acetone, and finally dried at 85 °C overnight (yield = 70%). Characterization details can be found in the Supporting Information.

General Synthesis of the PSM of UiO-66-NH_2. A 0.150 g portion of UiO-66-NH_2 (0.085 mmol) was suspended in ethanol (15 mL), and the corresponding aldehyde (4PC, 2PC, and Sal) was added to the dispersion. The resulting reaction mixture was then spray-dried at an inlet temperature of 130 °C, a feed rate of 3.0 mL min^{-1}, and a flow rate of 336 mL min^{-1} using a Mini Spray Dryer B-290 (BUCHI Labortechnik; spray cap: 0.5 mm hole). A yellow powder was collected after 5 min. The resulting solid was then dispersed in 20 mL of ethanol and precipitated by centrifugation. This process was repeated four times. The final product was washed one time with acetone and dried for 12 h at 85 °C. In addition, as a control experiment, the above-mentioned method was reproduced, except that, instead of spray drying the reaction mixture, we heated it at 130 °C for 5 min. Under these conditions, a conversion rate of only 3% was found. Full experimental and characterization details can be found in the Supporting Information.

General Synthesis of the PSM of ZIF-90. A dispersion of ZIF-90 (0.100 g, 0.39 mmol) and the corresponding amine in 15 mL of ethanol was spray-dried at an inlet temperature of 130 °C, a feed rate of 3.0 mL min^{-1}, and a flow rate of 336 mL min^{-1} using a Mini Spray Dryer B-290 (BUCHI Labortechnik; spray cap: 0.5 mm hole). A yellow powder was collected after 5 min. The resulting solid was then dispersed in 20 mL of ethanol and precipitated by centrifugation. This process was repeated five times. The final product was washed one time with acetone and dried for 12 h at 85 °C. In addition, as a control experiment, the above-mentioned method was reproduced, except that, instead of spray drying the reaction mixture, we heated it at 130 °C for 5 min. Under these conditions, the conversion rate was 0%. Full experimental and characterization details are reported in the Supporting Information.

Quantification Protocol. Samples were digested in strong acidic conditions, and their ^{1}H NMR spectra were collected to calculate the conversion of imine by the comparison of the integration of the characteristic signals of the corresponding reactants (amine and aldehyde). For the PSM of UiO-66-NH_2, 10 mg of activated sample,

DOI: 10.1021/jacs.6b11240
J. Am. Chem. Soc. 2017, 139, 897−903

0.6 mL of DMSO-d_6, and 120 μL of HF 5% were poured in a plastic NMR tube, and the mixture was sonicated for 1 h until a clear solution was obtained. For the PSM of ZIF-90, 10 mg of sample was digested with 20 μL of DCl and 0.75 mL of DMSO-d_6.

■ ASSOCIATED CONTENT

Supporting Information

The Supporting Information is available free of charge on the ACS Publications website at DOI: 10.1021/jacs.6b11240.

Experimental procedures and characterization data (PDF)

■ AUTHOR INFORMATION

Corresponding Author

*daniel.maspoch@icn2.cat

ORCID

Daniel Maspoch: 0000-0003-1325-9161

Notes

The authors declare the following competing financial interest(s): The authors have a patent pending on the methods described in this manuscript.

■ ACKNOWLEDGMENTS

This work was supported by the EU FP7 ERC-Co 615954 and European Union's Horizon 2020 research and innovation program under grant agreement No. 685727. I.I. thanks the MINECO for the RyC fellowship RyC-2010-06530. ICN2 acknowledges the support of the Spanish MINECO through the Severo Ochoa Centers of Excellence Program, under Grant SEV-2013-0295.

■ REFERENCES

(1) Furukawa, H.; Ko, N.; Go, Y. B.; Aratani, N.; Choi, S. B.; Choi, E.; Yazaydin, A. Ö.; Snurr, R. Q.; O'Keeffe, M.; Kim, J.; Yaghi, O. M. *Science* **2010**, *329*, 424.

(2) Horcajada, P.; Gref, R.; Baati, T.; Allan, P. K.; Maurin, G.; Couvreur, P.; Férey, G.; Morris, R. E.; Serre, C. *Chem. Rev.* **2012**, *112*, 1232.

(3) Carné, A.; Carbonell, C.; Imaz, I.; Maspoch, D. *Chem. Soc. Rev.* **2011**, *40*, 291.

(4) Evans, J. D.; Sumby, C. J.; Doonan, C. J. *Chem. Soc. Rev.* **2014**, *43*, 5933.

(5) Doonan, C. J.; Morris, W.; Furukawa, H.; Yaghi, O. M. *J. Am. Chem. Soc.* **2009**, *131*, 9492.

(6) Kim, M.; Cahill, J. F.; Prather, K. A.; Cohen, S. M. *Chem. Commun.* **2011**, *47*, 7629.

(7) Garibay, S. J.; Cohen, S. M. *Chem. Commun.* **2010**, *46*, 7700.

(8) Kim, M.; Cohen, S. M. *CrystEngComm* **2012**, *14*, 4096.

(9) Kandiah, M.; Usseglio, S.; Svelle, S.; Olsbye, U.; Lillerud, K. P.; Tilset, M. *J. Mater. Chem.* **2010**, *20*, 9848.

(10) Hou, J.; Luan, Y.; Tang, J.; Wensley, A. M.; Yang, M.; Lu, Y. *J. Mol. Catal. A: Chem.* **2015**, *407*, 53.

(11) Pintado-Sierra, M.; Rasero-Almansa, A. M.; Corma, A.; Iglesias, M.; Sánchez, F. *J. Catal.* **2013**, *299*, 137.

(12) Rasero-Almansa, A. M.; Corma, A.; Iglesias, M.; Sanchez, F. *Green Chem.* **2014**, *16*, 3522.

(13) Tang, J.; Dong, W.; Wang, G.; Yao, Y.; Cai, L.; Liu, Y.; Zhao, X.; Xu, J.; Tan, L. *RSC Adv.* **2014**, *4*, 42977.

(14) Wang, J.; Yang, M.; Dong, W.; Jin, Z.; Tang, J.; Fan, S.; Lu, Y.; Wang, G. *Catal. Sci. Technol.* **2016**, *6*, 161.

(15) Liu, J.; Zhang, X.; Yang, J.; Wang, L. *Appl. Organomet. Chem.* **2014**, *28*, 198.

(16) Saleem, H.; Rafique, U.; Davies, R. P. *Microporous Mesoporous Mater.* **2016**, *221*, 238.

(17) Morris, W.; Doonan, C. J.; Furukawa, H.; Banerjee, R.; Yaghi, O. M. *J. Am. Chem. Soc.* **2008**, *130*, 12626.

(18) Jones, C. G.; Stavila, V.; Conroy, M. A.; Feng, P.; Slaughter, B.; Ashley, C. E.; Allendorf, M. D. *ACS Appl. Mater. Interfaces* **2016**, *8*, 7623.

(19) Thompson, J. A.; Brunelli, N. A.; Lively, R. P.; Johnson, J. R.; Jones, C. W.; Nair, S. *J. Phys. Chem. C* **2013**, *117*, 8198.

(20) Liu, C.; Liu, Q.; Huang, A. *Chem. Commun.* **2016**, *52*, 3400.

(21) Servalli, M.; Ranocchiari, M.; Van Bokhoven, J. A. *Chem. Commun.* **2012**, *48*, 1904.

(22) Carné-Sánchez, A.; Imaz, I.; Cano-Sarabia, M.; Maspoch, D. *Nat. Chem.* **2013**, *5*, 203.

(23) Garzón-Tovar, L.; Cano-Sarabia, M.; Carné-Sanchez, A.; Carbonell, C.; Imaz, I.; Maspoch, D. *React. Chem. Eng.* **2016**, *1*, 533.

(24) Nguyen, J. G.; Cohen, S. M. *J. Am. Chem. Soc.* **2010**, *132*, 4560.

(25) Canivet, J.; Aguado, S.; Daniel, C.; Farrusseng, D. *ChemCatChem* **2011**, *3*, 675.

(26) Aguado, S.; Canivet, J.; Farrusseng, D. *Chem. Commun.* **2010**, *46*, 7999.

(27) Marti, A. M.; Tran, D.; Balkus, K. J. *J. Porous Mater.* **2015**, *22*, 1275.

(28) Ragon, F.; Horcajada, P.; Chevreau, H.; Hwang, Y. K.; Lee, U. H.; Miller, S. R.; Devic, T.; Chang, J.-S.; Serre, C. *Inorg. Chem.* **2014**, *53*, 2491.